J Electr Eng Technol Vol. 9, No. 3: 882-887, 2014
http://dx.doi.org/10.5370/JEET.2014.9.3.882

ISSN(Print) 1975-0102
ISSN(Online) 2093-7423

Thermal Analysis of IPMSM with Water Cooling Jacket for Railway Vehicles

Chan-Bae Park†

Abstract – In this paper, the water cooling method among the forced coolant cooling methods is considered to be applied to the 110kW-class IPMSM for railway vehicles. First, basic thermal property analysis of the IPMSM is conducted using the three-dimensional thermal equivalent network method. Then, based on the results of the basic thermal property analysis, some design requirements for the water cooling jacket are deduced and a basic design of the water cooling jacket is carried out. Finally, thermal equivalent circuit of the water cooling jacket is attached to the IPMSM's 3D thermal equivalent network and then, the basic thermal and effectiveness analysis are conducted for the case of applying the water cooling jacket to the IPMSM. In the future, the thermal variation trends inside the IPMSM by the application of the water cooling jacket is expected to be quickly and easily predicted even at the design step of the railway traction motor.

Keywords: Interior permanent magnet synchronous motor, IPMSM, Water cooling jacket, Thermal analysis, Thermal equivalent network

1. Introduction

The traction motor for the railway vehicle is installed on the axles of the bogie which is located on the lower part of the vehicle. Due to influence of the rail track environment, there is a large amount of dust blown during vehicle operations. Because of such operating environments, a totally-enclosed motor is primarily applied which can fundamentally block entry of any foreign substance from outside into the traction motor. However, the totally-enclosed motor, which has a problem for cooling, is not a suitable structure for the Interior Permanent Magnet Synchronous Motor (IPMSM) which has a permanent magnet embedded in the rotor. Especially, in recent market, where the downsizing of the traction motor both in size and weight is greatly in demand, research on a separate cooling device for the IPMSM is need to have a competitive edge.

In general, there are three cooling methods for the traction motor: natural air-cooling, forced air-cooling, and forced coolant cooling [1]. Of these, forced coolant cooling has the best cooling capacity. The smallest-sized traction motor is able to be designed if forced coolant cooling is applied to the IPMSM. However, for the application to be possible, research on the following is essential: 1) prediction of heat generated from inside the IPMSM which is designed to have high current density, 2) design of cooling channel and device to efficiently discharge the heat generated inside the IPMSM to the outside, and 3) a heat analysis technique to predict the cooling capacity of the designed cooling channel and device [1]. Fig. 1 shows recent trends of R&D on the railway vehicle's traction motor. Whereas there was research on the induction motor using natural air-cooling in the past, the direction of research has now changed into the IPMSM with water-cooling jacket. Therefore, in this paper, the water cooling method among the forced coolant cooling methods is considered to be applied to the 110kW-class IPMSM. First, basic thermal property analysis of the IPMSM is conducted using the three-dimensional (3D) thermal equivalent network method (TENM). Then, based on the results of the basic thermal property analysis, some design requirements for the water cooling jacket are deduced and a basic design of the water cooling jacket is carried out. Finally, thermal equivalent circuit of the water cooling jacket is attached to the IPMSM's 3D thermal equivalent network (TEN). Then, the basic thermal and effectiveness analysis are conducted for the case of applying the water cooling jacket to the IPMSM.

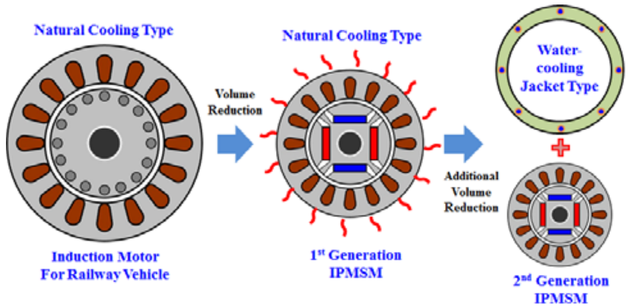

Fig. 1. Recent R&D trend of traction motor for railway vehicles

† Corresponding Author: Railroad Propulsion System Research Team, Korea Railroad Research Institute, Korea (cbpark@krri.re.kr)
Received: September 24, 2013; Accepted: November 28, 2013

Table 1. Main specifications of 110 kW-class IPMSM

Contents	Value	Unit
Slots / Poles	9 / 6	-
IPMSM Size	Dia. 316 / Stack 280	mm
Average torque (2400/6000rpm)	433.3 / 142.3	Nm
Iron loss (2400/6000rpm)	1.245 / 1.768	kW
PM eddy current loss (2400/6000rpm)	0.238 / 3.010	kW
Copper loss (2400/6000rpm)	1.052 / 1.052	kW
Output Power (2400/6000rpm)	110 / 89	kW

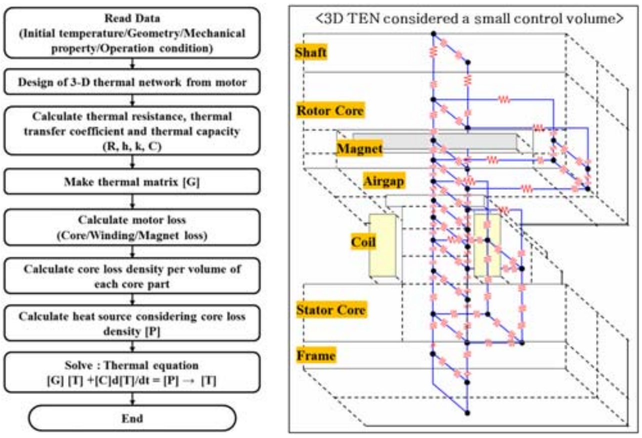

Fig. 2. Concept of thermal analysis of IPMSM and 3-D thermal equivalent network model

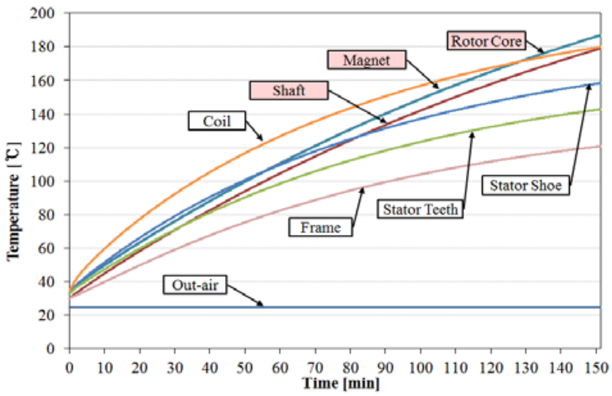

Fig. 3. Temperature rising properties of 110 kW-class IPMSM model (2400rpm)

2. Basic Thermal Property Analysis of the IPMSM

Thermal analysis is conducted for the 110kW-class IPMSM model by organizing 3D TEN. For the thermal analysis of the IPMSM, the overall heat distribution and flow of the IPMSM are identified by employing the lumped parameter method. When deducing heat sources such as thermal losses at each part of the heat equivalent circuit, a hybrid process using the distributed parameter method is applied [2]. Fig. 2 shows the thermal analysis concept of the IPMSM and 3D TENM proposed in this paper [3]. As shown in Fig. 2, 3D TEN considered a small control volume of the IPMSM is derived. Based on shapes and materials of each control volume of the IPMSM, the main thermal transfer coefficients (conduction/convection coefficients) are derived. The results are summarized in Table 2 [4]. Fig. 3 shows the transient thermal analysis results of the IPMSM at rated operation (2400rpm). As shown in Fig. 3, even with a relatively short time of operation, the temperature at each part of the IPMSM increases drastically. This is because the IPMSM is a totally-enclosed model without any cooling method, and the channel to forcefully discharge the heat, which has been generated inside the IPMSM, is not considered.

Table 2. Main thermal transfer coefficients of 110kW-class IPMSM

Contents			Thermal transfer coefficient [W/ m2℃]
	Components	Materials	
Conduction	Frame	Al6061	167
	Stator(Radial direction)	Si-steel(S08)	25
	Stator(Axial direction)	Si-steel(S08)	1.75
	Coil	Copper	398
	Rotor	Si-steel(S08)	25
	Magnet	NdFeB(N38EH)	7.6
	Shaft	Iron	50
Convection	Air-gap		65.04
	From frame to inner air / outer air		10 / 100
	From stator yoke / shoe to inner air		10 / 20
	From end-coil to inner air		15
	From rotor to inner air		20
	From magnet to inner air		20
	From shaft to inner air / outer air		10 / 17

3. Deduction of Specifications for a Water Cooling Jacket and Heat Transfer Properties

The cooling device for the IPMSM under consideration in this paper is a solenoid-typed water cooling jacket which covers the exterior of the stator core. According to the structure of the inner pipe, both 1-channel-type and 2-channel-type water cooling jackets are reviewed. Fig. 4 shows the structures of the water cooling jacket for the IPMSM. The following are the boundary conditions for analyzing the fluid movement and heat transfer properties inside the pipe of the water cooling jacket [5, 6]. i) The surrounding temperature of the pipe inside the water cooling jacket is uniform. ii) The inner surface of the pipe is smooth. iii) The flow speed inside the pipe is uniform regardless of position.

For the moment, this paper only considers a circular shape as the cross-section form of the pipe for water cooling. In the fluid inside the pipe, V_m is the average speed of the fluid. While fluid is flowing inside the water cooling jacket pipe with length L, the pressure drop is as shown in Eq. (1). Here, f is the friction coefficient and D is the diameter of the pipe. The pump power required to overcome a certain pressure drop of ΔP can be calculated by using Eq. (2); here, V is the volumetric flow rate that passes through the pipe. The friction coefficient and the heat transfer coefficient are higher at the pipe entry where the thickness of the boundary layer is 0, and gradually decrease inside the pipe. Therefore, the pressure drop and heat flux are higher at the pipe entry and improve the average friction coefficient and heat transfer coefficient throughout the entire pipe due to entry area effect. However, the entry area effect may be overlooked for long pipes. In circular pipes, the average Nu is given as shown in Eq. (3) for laminar flows. Here, Nu is the Nusselt number, Re is the Reynolds number, Pr is the Prandtl number, and μ_b and μ_s are the dynamic viscosity of fluid calculated on the average temperature and the surface temperature, respectively. The interaction formulas between friction factor, f, and Nu are given in Equations (4) and (5) in case of the completely developed turbulent flows in the smooth circular pipe.

$$\Delta P = f\frac{L}{D}\frac{\rho V_m^2}{2} \quad [N/m^2] \tag{1}$$

$$\dot{W}_{pump} = \dot{V}\Delta P = \frac{\dot{m}\Delta P}{\rho} \quad [W] \tag{2}$$

$$Nu = 1.86\left(\frac{\mathrm{Re}\,\mathrm{Pr}\,D}{L}\right)^{1/3}\left(\frac{\mu_b}{\mu_s}\right)^{0.14} \qquad (\mathrm{Pr} > 0.5) \tag{3}$$

$$f = (0.79\ln\mathrm{Re} - 1.64)^{-2} \qquad (3000 \le \mathrm{Re} \le 5\times10^6) \tag{4}$$

$$Nu = \frac{(f/8)(\mathrm{Re}-1000)\mathrm{Pr}}{1+12.7(f/8)^{0.5}(\mathrm{Pr}^{2/3}-1)} \qquad \left(\begin{array}{l}0.5 \le \mathrm{Pr} \le 2000 \\ 3000 \le \mathrm{Re} \le 5\times10^6\end{array}\right) \tag{5}$$

Table 3 shows the main specifications of the water cooling jacket for the 110kW-class IPMSM. The pipe material is copper with high heat conductivity. The total length of the pipe is 8.8(m) and both the 1-channel and 2-channel models are considered. Fig. 5 shows the analysis results of each characteristic parameter following changes in flow velocity of coolant inside the pipe of the water cooling jacket. Fig. 5 (a) shows changes to the Nusselt number. As shown in Fig. 5 (a), turbulence is generated even in slow flow velocity as the diameter of the pipe increases. On the other hand, if the pipe diameter is uniform regardless of pipe length, then the Nusselt number is consistent throughout. Fig. 5 (b) shows the exit temperature variations of the coolant. Since the surrounding temperature of the pipe is 75(℃), it would help in improving the thermal absorption of the coolant if the water cooling jacket is designed such that the exit temperature of the coolant would reach around 75(℃). For such a design, the case in which the flow inside the pipe is turbulent would be most effective, but the required thermal absorption of the pipe and the capacity of the coolant circulation pump would also have to be considered at the same time. Fig. 5 (c) shows changes in NTU. NTU is known as the net transfer unit and it is the index of a heat transfer system performance. In general, for a system with NTU greater than 5, it can be said that the system has overcome the heat transfer threshold [7, 8]. As shown in Fig. 5 (c), the shorter the pipe length or the bigger the pipe diameter, it is easier to design a system with NTU over 5. Fig. 5 (d) shows changes in the thermal absorption rate of

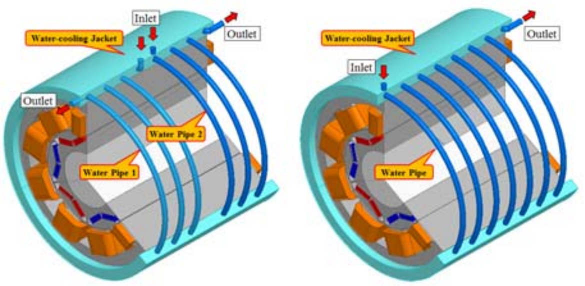

(a) 2-channel solenoid type (b) 1-channel solenoid type

Fig. 4. Water cooling jackets for 110kW-class IPMSM

Table 3. Main specifications of Water-cooling Jacket

Contents	Model I	Model II	Unit
Pipe material	Copper	Copper	-
Frame material	AL6061	AL6061	-
Total channel length	4.4*2ea (2 ch.)	8.8 (1 ch.)	m
Pipe diameter	5~10	5~10	mm
Inlet water temp.	20	20	℃
Surrounding temp. of pipe	75	75	℃

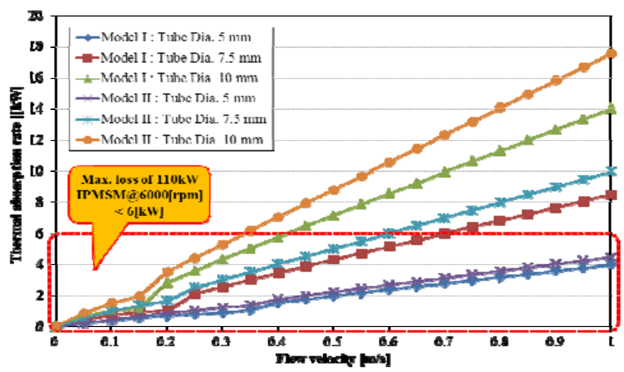

Fig. 5. Analysis results of characteristic parameters by flow velocity increasing on the inside of the pipe

Table 4. Design Results of Water-cooling Jacket for 110 kW-class IPMSM

Design contents	Results	Unit
Type	Model 2 (1 channel)	-
Channel(Pipe) Length	8.8	m
Pipe Diameter	10	mm
Water Flow Velocity Limit	0.35	m/s
Water Flow Capacity	1.65	l/min
Inlet Water Temperature	20	℃
NTU Limit	5	-
Outlet Water Temperature	75	℃
Thermal Absorption Rate Limit	6	kW
Pressure Drop of Pipe	2023	N/m^2
Pump Power	56	W

the coolant. As shown in Fig. 5 (d), the larger the pipe diameter, the higher the thermal absorption rate of the coolant, and using one pipe with a long channel yields a higher thermal absorption rate than using two pipes with short channels. Additionally, as the pipe diameter gets larger, the variation of the thermal absorption rate increases even with small changes in the flow velocity of the coolant. In areas where the coolant flow is turbulent, the thermal absorption rate is seen to drastically increase. Moreover, since the total sum of electromagnetic losses of the IPMSM, excluding mechanical loss, is about 5.83(kW), the thermal absorption of the water cooling jacket should be limited to 6(kW). Such limitation is also related to the pump capacity required for coolant circulation; thus, economic aspects should be considered as well [9, 10]. The design specifications of the water cooling jacket for the 110kW-class IPMSM are summarized in Table 4.

4. Thermal Analysis of 110kW-class IPMSM with the Water Cooing Jacket

4.1 Thermal analysis method of the IPMSM with the water cooling jacket using TENM

In this paper, TENM is employed to analyze the thermal property variations on the IPMSM when the water cooling jacket is applied. More specifically, variations in temperature and current density at the IPMSM coil by heat absorption of the water cooling jacket were analyzed.

The thermal analysis method using TEN for the 110kW-class IPMSM with the water cooling jacket is shown in Fig. 6. As shown in Fig. 6, the coolant flowing through the pipe inside the water cooling jacket acts as an absorbent of the heat surrounding the pipe. Thus, the absorption rate can be equalized to a heat source on the TEN. However, unlike the previous IPMSM TEN in which the losses generated from the stator, rotor, permanent magnet, and coil are input as (+) heat sources, the water cooling pipe of the water cooling jacket should be input as a (-) heat source since the pipe absorbs surrounding heat. To analyze thermal properties of the IPMSM with the water cooling jacket using TENM, it must be assumed that the thermal absorption rate of the coolant flowing through the pipe inside the water cooling jacket is consistent throughout. In Table 4, the total thermal absorption capacity of the water cooling jacket has been limited to 6(kW). Therefore, as shown in Fig. 6, if the water cooling jacket is divided into four control volume models in axial directions, then the jacket can be equalized to four (-) heat sources. Consequently, the thermal absorption capacity of each control volume reaches a maximum of approximately 1.25 (kW).

4.2 Thermal analysis results by applying the water cooling jacket

TEN of the 110kW-class IPMSM with the water cooling jacket is created by inserting the water cooling jacket model at the stator core exterior of the IPMSM. The flow velocity of the coolant is increased from 0 to 0.35(m/s) and the temperature variation property inside the IPMSM is predicted. First, as shown in Fig. 3, after 150 minutes of operation without the application of the water cooling jacket, the temperatures of the IPMSM coil, the frame and the permanent magnet reached about 180(℃), 121(℃), 187(℃), respectively. Fig. 7 shows the temperature variation effects on the IPMSM model due to the increase in the coolant flow velocity upon application of the water-cooling jacket. As shown in Fig. 7, the temperature at all parts inside the IPMSM drops as the flow velocity of the water cooling jacket is increased from 0 to 0.35(m/s). Especially, the temperatures at the stator and coil experience a much greater drop than the rotor since these parts are in direct contact with the water cooling jacket. Additionally, when the flow velocity exceeds 0.2(m/s), the flow inside the pipe changes from laminar to turbulent, and the thermal absorption rate and temperature drop rate increase due to coolant. Fig. 8 shows the property variations on the coil of the IPMSM model

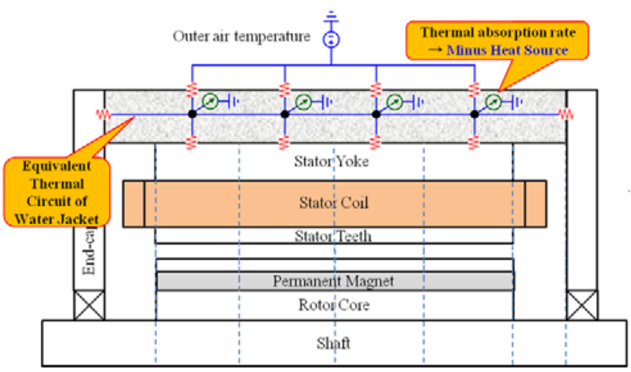

Fig. 6. Analysis methods by thermal equivalent network when water-cooling jacket is applied to 110kW-class IPMSM

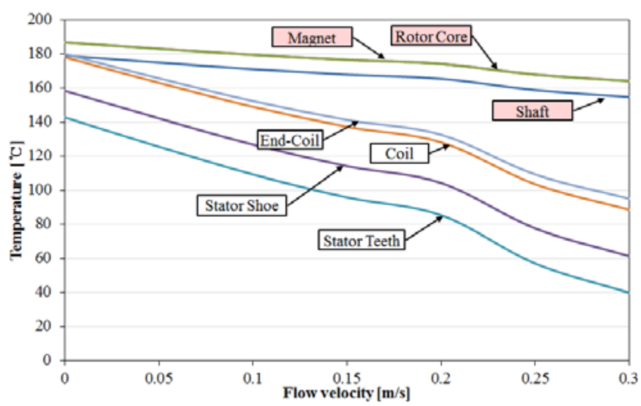

Fig. 7. Temperature variation properties of 110kW-class IPMSM model due to the increase of the coolant flow velocity on the water-cooling jacket

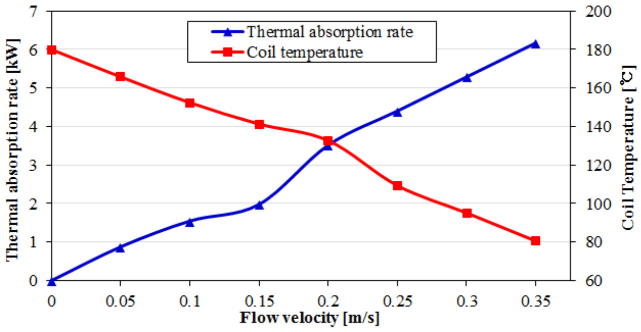

(a) Thermal absorption rate & coil temperature

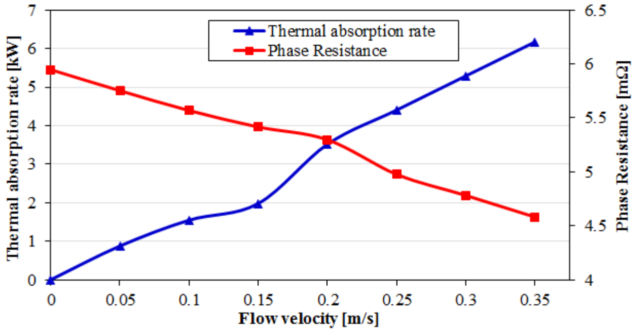

(b) Thermal absorption rate & phase resistance

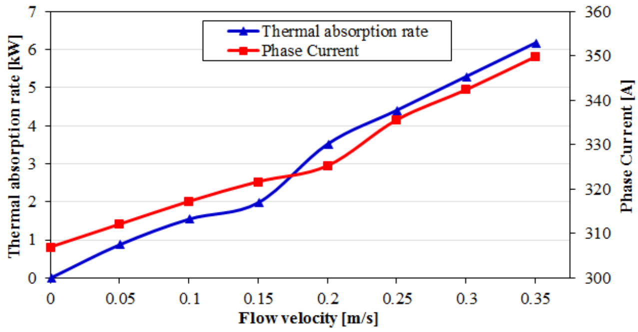

(c) Thermal absorption rate & winding phase current

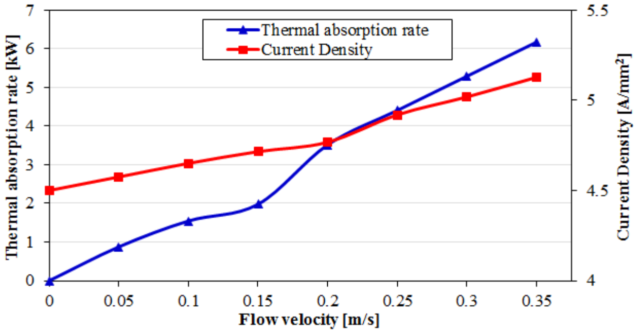

(d) Thermal absorption rate & winding current density

Fig. 8. Properties variations on the winding of 110kW IPMSM-class model due to the increase of the coolant flow velocity on the water-cooling jacket

due to the increase in coolant flow velocity on the water cooling jacket. Fig. 8 (a) shows the property variation between the thermal absorption rate of the water cooling jacket and the temperature of the coil due to the increase of the coolant flow velocity. When the flow velocity is increased up to 0.35(m/s), the coil temperature drops from 180(℃) to 95.1(℃). This is approximately an 85(℃) drop. Fig. 8 (b) and (c) show the property variation among the thermal absorption rate, phase resistance and phase current on the coil. When the flow velocity is increased up to 0.35(m/s), the phase resistance drops from 5.95(mΩ) at 180(℃) to 4.78(mΩ) by approximately 1.17(mΩ) by the temperature drop of the coil. Consequently, the phase current margin of about 35.4(A) from 307(A) at 180(℃) to 342.4(A) can be obtained. Fig. 8 (d) shows the property variation between the thermal absorption rate and the current density of the coil. When the flow velocity is increased up to 0.35(m/s), it can be predicted that the current density of the coil is increased by approximately 0.52(A/mm^2) from 4.5(A/mm^2) to 5.02(A/mm^2). According to the analysis results, the phase resistance decrease of approximately 32(%) is generated because of the temperature drop of the coil caused by the thermal absorption of the water cooling jacket. The decrease in the phase resistance in turn leads to an increase in the coil current density by approximately 21(%).

In conclusion, the thermal analysis method of the 110 kW-class IPMSM model with the thermal model of the water cooling jacket using the 3D TENM is presented in this paper, and the temperature variation trends inside the IPMSM by the application of the water cooling jacket can be quickly and easily predicted even at the design step of the railway traction motor.

5. Conclusion

Water cooling jackets have yet to be applied to any traction motors for railway vehicles in Korea. Thus, this paper handled to conduct basic design of a water cooling jackets and also investigate heat transfer properties. The 3D TENM for the 110 kW-class IPMSM is first employed to conduct a basic thermal property analysis. After analyzing the basic thermal properties of the IPMSM, the necessary specifications for the water cooling jacket were deduced based on the thermal analysis results of the IPMSM. Next, heat transfer properties were analyzed by using an equivalent model of the solenoid-typed pipe which is to be installed within the water cooling jacket of the IPMSM. A basic design model for the 6 kW-class water cooling jacket was deduced. Finally, thermal equivalent circuit of the water cooling jacket was attached to the IPMSM's 3D TEN, and the basic thermal and effectiveness analysis were conducted for the case of applying the water cooling jacket to the IPMSM. In future studies authors intend to make a 6 kW-class water cooling jacket and a 110 kW-class IPMSM and to validate the proposed design and thermal analysis method of the water cooling jacket with the IPMSM.

References

[1] A. F. Armor, and M. V. K. Chari, "Heat flow in the stator core of large turbine-generators by the method of three dimensional Finite Elements (Part II: Temperature distribution in the stator iron)," *IEEE Transactions on PAS*, PAS-95(5), pp. 1657-1668, 1976.
[2] C. B Park, H.W. Lee, B. S. Lee, "A Study on the Reduction of the Stator Iron Loss on Permanent Magnet Synchronous Motor for light Railway Transit Propulsion System," *Journal of the Korean Society for Railway*, Vol.15, No.4, pp. 376-380, 2012.
[3] C. B Park, H.W. Lee, B. S. Lee, "Investigation of a thermal analysis method for IPMSM in railway vehicles," *Journal of the Korean Society for Railway*, Vol.16, No.2, pp. 99-103, 2013.
[4] C. B. Park, "A Study on the Thermal Characteristics of 110kW-class IPMSM for Light Railway Transit using the 3-Dimensional Thermal Equivalent Network considering Heat Source by Iron Loss Density Distributions," *The transactions of the Korean Institute of Electrical Engineers*, Vol. 62, No. 7, pp. 1038-1044, 2013.
[5] Y. Bayazitoglu and M. N. Ozisik, "Element of Heat Transfer." New York : McGraw-Hill, 1988.
[6] F. Kreith and M.S. Bohn, "Principles of Heat Transfer: 5th edition," St. Paul, MN : West Publishing, 1993.
[7] T. Jokinen and J. Saari, "Modeling of the coolant flow with heat flow controlled temperature sources in thermal networks," *IEE Proceeding of Electrical Power Applications*, Vol.144, No.5, 1997.
[8] J.H. Choi, S.M. Jang, C. Han, J.H. Ahn, K.H. Sim, "Electromagnetic loss and thermal analysis on high speed PM motor for turbo compressor," *KIEE Summer Conference 2012*, pp. 618-619, 2012.
[9] J. Driesen, R. J. M. Belmans, and K. Hameyer, "Finite-element modeling of thermal contact resistances and insulation layers in electrical machines," *IEEE Transactions on Industry Applications*, Vol.37, No.1, pp. 15-20, 2001.
[10] Batchelor, G. K., "An Introduction to Fluid Dynamics," Cambridge University Press, 1967.

Chan-Bae Park He received his M.S. degree in Electrical Engineering from Seoul National University, Seoul, Korea, in 2003, and the Ph.D. degree in electrical engineering from Hanyang University, Seoul, Korea, in 2013. Since 2007, he has been a Senior Researcher at Korea Railroad Research Institute, Uiwang, Korea. His research interests include design and analysis of motor/generator, wireless power transfer system, and superconducting devices for energy conversion systems.